

Transactivation of Abl by the Crk II adapter protein requires a PNAV sequence in the Crk C-terminal SH3 domain

Charles Reichman¹, Kamalendra Singh¹, Yan Liu¹, Sukhwinder Singh¹, Hong Li¹, J Eduardo Fajardo², Andras Fiser² and Raymond B Birge^{*1}

¹Department of Biochemistry and Molecular Biology, UMDNJ-New Jersey Medical School, 185 South Orange Avenue, Newark, NJ 07103, USA; ²Department of Biochemistry, Albert Einstein College of Medicine, Bronx, NY 10461, USA

To gain a better understanding of how Crk II regulates the function of the Abl tyrosine kinase, we explored the function of the C-terminal linker and SH3 domain, a region of Crk II that is still poorly understood. Molecular modeling, tryptophan fluorescence, and covariation sequence alignment indicate that the Crk-SH3-C has a unique binding groove and RT loop not observed in typical SH3 domains. Based on these models, we made a series of mutations in the linker and in residues predicted to destabilize the putative binding pocket and RT loop. In Abl transactivation assays, Y222F and P225A mutations in the linker resulted in strong transactivation of Abl by Crk II. However, mutations predicted to be at the surface of the Crk SH3-C were not activators of Abl. Interestingly, combinations of activating mutations of Crk II with mutations in the highly conserved PNAV sequence in the SH3-C inactivated the activating mutations, suggesting that the SH3-C is necessary for activation. Our data provide insight into the role of highly conserved residues in the Crk-SH3-C, suggesting a mechanism for how the linker and the Crk-SH3-C function in the transactivation of the Abl tyrosine kinase.

Oncogene (2005) 24, 8187–8199. doi:10.1038/sj.onc.1208988; published online 12 September 2005

Keywords: Crk; Abl; SH3 domain; atypical; covariation; protein modeling; kinase activation

Introduction

The Crk II protein is an SH2–SH3 domain containing adapter protein involved in cytoskeletal reorganization and events associated with cellular adhesion, migration, phagocytosis, cellular proliferation, and oncogenic transformation (Feller, 2001). Crk II, the cellular homolog of the v-Crk oncoprotein, is expressed from two alternatively spliced mRNAs to produce Crk II (p38) and Crk I (p28). Crk II and Crk I differ in their C-terminal regions (Matsuda *et al.*, 1992; Reichman *et al.*, 1992; Feller, 2001). Crk II contains an N-terminal SH2 domain and two SH3 domains (SH3-N and SH3-C).

Crk II also contains an approximately 45 amino-acid linker between the two SH3 domains. In contrast, v-Crk and Crk I encode proteins with C-terminal truncations that do not possess a regulatory tyrosine residue 222 (Y222) between the SH3 domains, or the C-terminal SH3 domain (Mayer *et al.*, 1988; Reichman *et al.*, 1992). Expression of v-Crk or Crk I in cells robustly increases cellular phosphotyrosine levels, and transforms cells, despite the fact that neither protein has intrinsic tyrosine kinase activity. While several cellular proteins have been identified that bind to the SH2 and SH3-N domain, Abl and its paralog Arg are the only tyrosine kinases that are known to directly associate with v-Crk or Crk II (Feller *et al.*, 1994; Ren *et al.*, 1994; Wang *et al.*, 1996). Binding of v-Crk or Crk I to Abl results in Abl transactivation, and possibly contributes to the transforming potential of Abl (Ren *et al.*, 1994; Sattler and Salgia, 1998; Hemmeryckx *et al.*, 2002). In contrast, the Crk II–Abl interaction is more transient, and by a signal that is not well understood, Abl-bound Crk becomes phosphorylated on Y222 by the Abl kinase, resulting in the intramolecular association of Y222 with the Crk SH2 domain, and dissociation of Crk from Abl (Feller *et al.*, 1994; Rosen *et al.*, 1995). Expression of Y222F Crk II enhances Abl transactivation, increases cellular phosphotyrosine, and promotes cellular transformation (Shishido *et al.*, 2001; Zvara *et al.*, 2001). Presently, the molecular mechanism by which Crk II activates Abl is not well understood, although previous studies suggest that the SH2 and SH3-C domains are necessary (Shishido *et al.*, 2001). The present study was carried out to investigate the structural and functional characteristics of the Crk-SH3-C. We present data that the linker and the Crk-SH3-C, through conserved residues in the modeled binding pocket and RT loop of the SH3-C, play important roles in the transactivation of the Abl tyrosine kinase.

Results and discussion

Threading analysis, computational molecular modeling, and biophysical studies of the C-terminal Crk SH3 domain (Crk SH3-C)

Previous efforts to identify binding partners of the Crk-SH3-C domain failed to detect an interaction with

*Correspondence: RB Birge; E-mail: birgera@umdnj.edu
Received 2 March 2005; revised 23 June 2005; accepted 24 June 2005;
published online 12 September 2005

canonical PxxPxK,R containing motifs. Feller *et al.* (1994) previously reported that the Crk-SH3-N, but not the Crk-SH3-C, bound Abl. It has also been demonstrated that the Crk-SH3-N can interact with PXXPK motifs from C3G, whereas Crk-SH3-C cannot (Knudsen *et al.*, 1994). Using a ³⁵S peptide overlay assay (Feller *et al.*, 1995), Crk-SH3-N was shown to bind to a number of cellular proteins, although no binding partners of Crk-SH3-C were detected. We also failed to detect Crk-SH3-C binding to a PPPALPPKK peptide by tryptophan fluorescence (data not shown). It has been reported, however, that the Crk-SH3-C can bind to the nuclear export protein Crm1 (Smith *et al.*, 2002).

To define the structural elements of the Crk-SH3-C and ascertain whether its structure conforms to that of canonical SH3 domains, we utilized unbiased threading analysis, sequence alignment, template structure-based modeling, and tryptophan fluorescence spectroscopy on purified recombinant proteins in the present paper. We employed an unbiased threading analysis to determine structures in the databases that most closely match the structure of the Crk-SH3-C (aa 239–293). Threading analysis (using Fugue and 3D-PSSM databases) identified several structures, all SH3 domains (Figure 1a), and 10 models were built on each selected structure. The best model produced, based on the evaluations performed with Prosa, was one based on the crystal structure of the SH3-C domain of human Grb2 (Lowenstein *et al.*, 1992), an SH2/SH3 domain containing adapter protein. High-quality models were also produced from the SH3

domains of *Caenorhabditis elegans* Sem-5 (Rozakis-Adcock *et al.*, 1992), and of the mouse Grb2-like protein Mona/Gads (Lewitzky *et al.*, 2004). All are atypical SH3 domains that bind PXXP-independent motifs. Crk-SH3-C also had structural similarities to p47phox, the Vav proto-oncogene SH3-N, and Amphiphysin II (Figure 1a). Based on the threading, the best template we found was Grb2-SH3-C (1gri). Therefore, we built the homology model using Grb2-SH3-C as a template. However, the homology-based model using the N-terminal SH3 domain of Crk superimposed on the one built with Grb-2 SH3-C had an RMS deviation of 1.73 Å. This suggests that models built on either template could be used for comparison purposes to Crk SH3-C, and for further analysis.

We wanted to explore how the SH3-C might differ in its structure and peptide-binding activity from those of canonical SH3 domains. Since the binding pocket of the Crk-SH3-N is well established to bind conventional PXXP peptide-containing proteins, the minimal energy molecular modeling program Look (version 3.5) was employed to model the structure of the SH3-C using the crystal structure of mouse Crk SH3-N bound to an interacting peptide as the template. The SH3-N interacting peptide is PPPALPPKK, from the Crk interacting protein C3G (Wu *et al.*, 1995). The predicted structure of Crk SH3-C is consistent with conventional SH3 domains, comprising five antiparallel β sheets, and two flexible variable loops called the RT loop and a 3₁₀ turn between the fourth and fifth β sheets that flank a

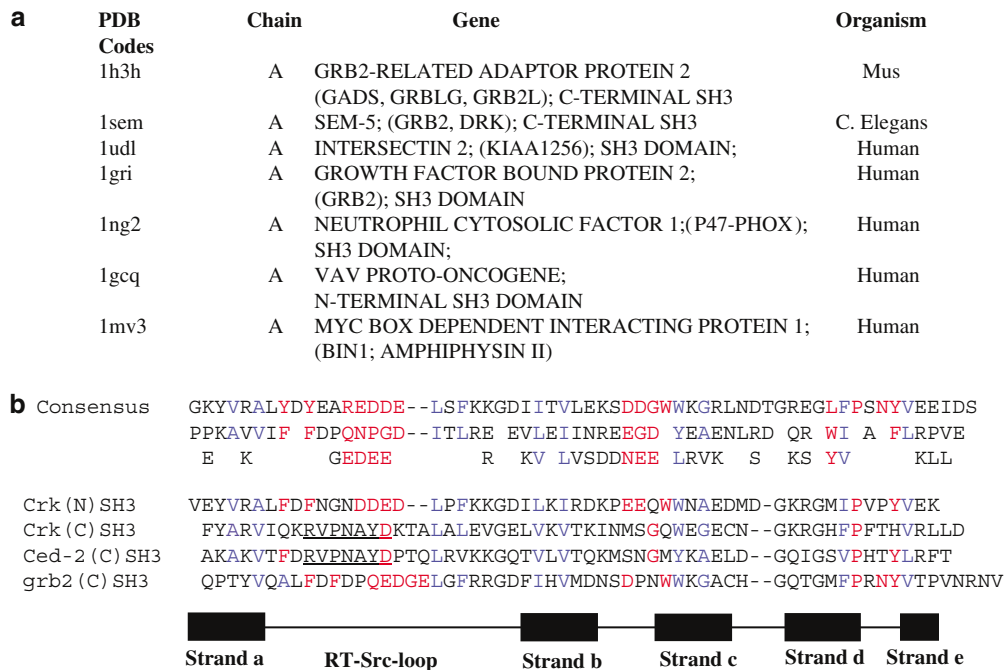


Figure 1 Sequence alignment and threading analysis. (a) Structures identified by threading analysis as suitable templates for modeling the Crk-SH3-C domain. The PDB code, chain, a brief description of the chain, and the source organism are provided. (b) The SH3 consensus sequence as determined by the covariation analysis of Larson and Davidson (2000) (*op cit*) was aligned with the Crk SH3-N, Crk SH3-C and human Grb2 SH3-C using Clustal W software; blue = hydrophobic core residues; red = binding to PXXPK/R. Note that in Crk-SH3C and Ced-SH3C, the canonical peptide-binding amino acids are poorly conserved. Underlined residues = short, identical region in Ced-2 and Crk SH3-C

possible binding pocket (Figure 2a). Superimposition of the modeled N- and C-terminal Crk SH3 domains, while indicating subtle differences between the RT loop and β c and β d loops, nevertheless suggests an overall conservation of structure between the two SH3 domains (Figure 2a). Moreover, while only 17% identical to the mammalian proteins, the model of the Ced-2 SH3-C also had the basic β -barrel structure characteristic of all SH3 domains, when modeled using the SH3-N of Crk II as the template. It may fold in order to generate a modular domain (data not shown).

Covariation analysis of protein sequences involves the study of statistical variations in amino-acid sequences in homologous proteins or protein domains, and analyzes whether a change in an amino acid at one position correlates with a change at another site in the protein. If such covarying sites are found, then it is hypothesized that these two sites likely interact in some manner, for example by contributing to the overall tertiary structure, or to a complex binding region. Using covariation analysis of 266 SH3 domains, consensus sequences for

SH3 domains have been derived. Two types of amino acids have been identified in the consensus sequence, those conserved for folding into the SH3 hydrophobic core, and those typically present at the surface and conserved for interaction with PXXP containing peptides (Larson and Davidson, 2000; Larson *et al.*, 2000).

We compared the SH3 domains of Crk II, Ced-2, and the Grb2 SH3-C to the SH3 consensus sequence derived by Larson *et al.* (2000). As illustrated in Figure 1b, Crk SH3-C and Ced-2-SH3-C are remarkably conserved in the hydrophobic core residues that maintain the overall tertiary structure of SH3s (10/10 hydrophobic core amino acids are either identical or conserved in Crk II and 9/10 in Ced-2). In contrast, Crk SH3-C and Ced-2 SH3-C had a general lack of conservation in the peptide-binding surface, whereby only three of 16 amino acids were conserved in Crk II and five of 16 in Ced-2. Even Grb2-SH3-C, which had the most similar structure to Crk II as evidenced by the threading analysis, had more conservation in the peptide-binding amino acids, compared to Crk-SH3-C (Figure 1b).

We performed tryptophan measurements on recombinant Crk SH3-C domain proteins. While most SH3 domains contain a contiguous tryptophan duet (WW) in the c strand, the Crk SH3-C domain contains a single tryptophan (W276). This fact led us to test whether this Trp is unconstrained (unfolded, $E_{max} \sim 353\text{--}360$ nM) or constrained ($E_{max} \sim 333\text{--}342$ nM). As shown in Figure 2b, Trp fluorescence measurements of the full-length SH3 domain (aa 239–293) or the SH3 domain containing parts of the linker-C-terminal SH3 domain had E_{max} values of $\sim 339\text{--}342$ nM, consistent with a folded polypeptide structure. Another N-terminal truncated linker-SH3C protein (aa 230–293), and an SH3-C protein comprising aa 239–297, also had a similar E_{max} (data not shown). Finally, we generated an N-terminal truncated SH3-C domain (Δ FYARVIQ) that deletes the first seven amino acids in the putative β 1 SH3 strand (Crk Δ SH3-C). This generates a protein with E_{max} of ~ 358 nM, consistent with an unfolded, denatured structure (Figure 2b). These data do not contradict the model of the SH3-C.

The vast majority of SH3 domains recognize specific proline-rich sequences that adopt the conformation of polyproline type I or type II helices (PPII), containing the core sequence PXXP (Kay *et al.*, 2000). In typical SH3 domains, the PXXP core motif is stabilized by stacking of the aromatic residues, Trp, Phe, and Tyr, which interact directly with the pyrrolidine rings of the PXXP. Additional binding specificity occurs outside of this core interaction and confers specificity among distinct SH3 domains. Recently, a number of SH3 domains have been reported to bind unconventional non-PXXP-dependent motifs in target proteins. Such examples include an RKXXYXXY motif in SKAP55 that binds the Fyn and Lck SH3 domains (Kang *et al.*, 2000), a PXXDY motif in several proteins that binds the Eps8 SH3 (Mongioli *et al.*, 1999), a WXXXFXXLE motif in p67phox and Pex5p that binds the Pex13p SH3 domain (Barnett *et al.*, 2000; Kami *et al.*, 2002), a PX(V/I)(D/N)RXXKP motif in Gab1 and SLP-76 proteins

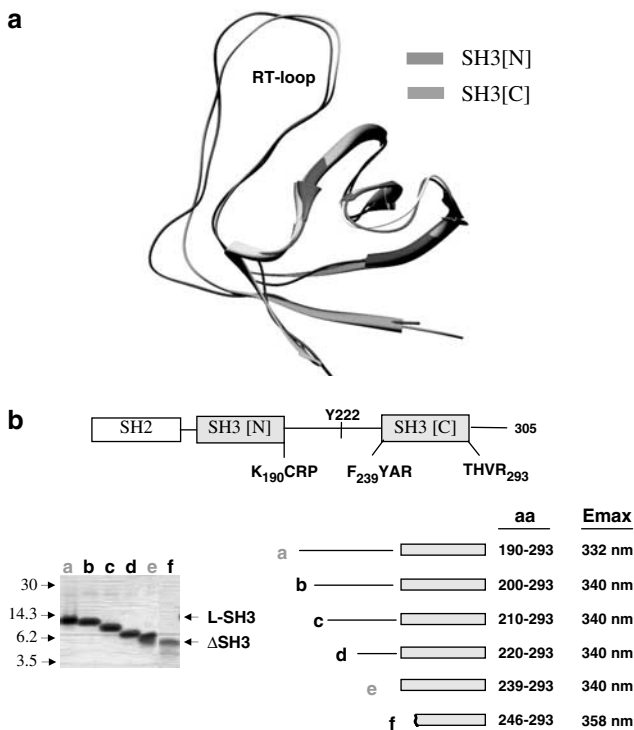


Figure 2 Basic SH3-C model and tryptophan fluorescence on recombinant proteins. (a) Ribbon structure of the Crk SH3-N (gray), superimposed on the modeled structure of the Crk SH3-C (dark gray). The RT loop is seen on the upper left. (b) Tryptophan fluorescence analysis of the SH3-C domain containing proteins. A linear map of Crk II depicting the linker region (aa 190–238) and SH3-C (aa 239–293), and the boundaries of linkerSH3-C peptides, (a) aa 190–293; (b) aa 200–293; (c) aa 210–293; (d) aa 220–293; (e) aa 239–293 (SH3-C domain), and (f) aa 246–293 (Δ SH3-C) are shown. At right in this panel are the normalized fluorescence of peptides a–f; at lower left is a Coomassie blue stained gel of the peptides, with size markers at left and SH3-C and Linker-SH3-C (L-SH3) at right. All proteins were analysed by mass spectrometry to verify mass

that bind the Mona/Gads SH3 domain (Lewitzky *et al.*, 2001; Harkiolaki *et al.*, 2003; Lewitzky *et al.*, 2004), and a PX(P/A)XXR motif that binds to the CIN85/SETA/Rut protein SH3 domains (Kurakin and Bredesen, 2002; Kurakin *et al.*, 2003). For some atypical SH3 domains, for example Mona/Gad, SKAP55, and Eps8, the unconventional peptides have been suggested to bind to regions including the classical PXXP binding site (Harkiolaki *et al.*, 2003). However, studies with Pex13p show that it can bind both conventional PXXP-containing peptides in the usual way, as well as a second, non-PXXP peptide, that binds at a novel, noncanonical pocket on the same SH3. Both peptides can bind to the Pex13p SH3 simultaneously (Pires *et al.*, 2003). Therefore, it would not be unprecedented to find an SH3 whose overall structure is similar to that of most other SH3s, but whose binding surface is very different, as we have presented evidence here concerning the SH3-C of Crk II.

The covariation analysis suggests that the binding residues of the SH3-C may be very different from those of canonical SH3s. As we show below, when the modeled SH3-C is superimposed on the template SH3-N and compared in detail, the potential peptide-binding residues of the SH3-C also look very different. For these reasons, we believe it is probable that the SH3-C of Crk II will be shown to be atypical in the peptides it can bind, and will likely not bind conventional PXXP peptides.

In order to predict which residues might occupy the binding surface of the SH3-C, and for later mutagenesis studies, we compared in detail the residues in the SH3-N peptide that made direct contact with P3, P6, and K8 positions of the PPPALPPKK peptide to the corresponding substituted amino acids in the SH3-C. The peptide residues at the P3, P6, and K8 positions of the interacting peptide are the most important because they conform to the PXXPK consensus sequence. There are a total of 12 residues in the Crk SH3-N domain within potential interacting distance (3.8 Å) of the C3G peptide (Figure 3). These residues are L140, F141, Y186, P185, P183, Q168, W169, E167, E166, D147, E149, and D150. The topologically equivalent residues in the modeled C-terminal Crk SH3 domain are K246, R247, H291, T290, P288, G274, Q275, S273, M272, D253, T255, and A256. Some of these are illustrated in Figure 3. If the region in the SH3-C model analogous to the binding groove in the SH3-N also binds a peptide, the comparison of the properties of the binding site residues in the two domains suggests that the nature of the peptides that bind the two proteins are probably dissimilar. Interestingly, several of the hydrophobic residues in the N-terminal SH3 domain that make direct contact with the pyrrolidine rings of the PXXP motif are replaced with basic or polar amino acids in the model of the SH3-C. For example, F141 is replaced by K246 (Figure 3a), Y186 is replaced by H291 (Figure 3a), and W169 is replaced by Q275 (Figure 3b). Another major difference is the characteristics of the binding site for interacting residues with K8 and K9 of the peptide. The two lysine residues of the C3G peptide form

extensive salt bridges with negatively charged residues of the Crk SH3-N (Figure 3c; Wu *et al.*, 1995). K8 forms three ion pairs with D147, E149, and D150, and only one of the residues (equivalent to D147) is conserved in the SH3-C. The other two residues are replaced by a Thr (T255) and Ala (A256). Similarly, the possibility of the salt bridge between K9 and E167 of Crk SH3-N also does not exist in Crk SH3-C, because the equivalent position to E167 of the SH3-N is occupied by a Ser residue (not shown). These dissimilarities clearly establish the differences in the nature of recognized and bound peptides by the SH3-N versus the modeled structure of the SH3-C, and suggest that the Crk SH3-C does not bind conventional PXXP-containing ligands.

In Figure 3d, we show a space-filling model of the SH3-C, together with a peptide in the place analogous to the peptide binding groove of the SH3-N. Each of the similar regions that interact with P3, P6, and K8 in the SH3-N are highlighted in blue, green, and yellow, respectively. Note that a potential binding groove still exists where the peptide is positioned, although as detailed above, important specific interactions for PXXPK peptides are not present in the SH3-C model. Finally, we note that a portion of the RT loop of SH3-C has residues that point away from the SH3-C domain (red, Figure 3d), and because of this might be more available to interact with other molecules. These include R247 to T255. In a study of the structures of 17 SH3 domains, investigators noted the surprising presence of stabilizing interactions among residues of the RT-Src loop that are not directly involved in peptide binding. They speculated that these conserved interactions might stabilize the RT loop as a whole for interactions with other peptides (Larson and Davidson, 2000). The α positions of the SH3-C residues R247, V248, P249, A251, Y252, D253, and T255, and the corresponding residues in Ced-2 (oriented similarly) are highly conserved in a wide range of species of Crk and CrkL, including chicken, mammals, *Xenopus laevis*, *Drosophila melanogaster*, and *C. elegans* (Table 1). Later, we detail how we used a mutational analysis of residues in each of the four blocks highlighted in Figure 3d to understand the functions of the SH3-C. We did this by investigating how they affect the activation of the Abl tyrosine kinase by Crk II.

Contributions of the linker (aa 190–238) and the Crk-SH3-C to regulating the interaction between Abl and Crk

Previous studies have shown that Crk binding to Abl has a transactivating function, and therefore we can score the extent of Abl activation when coexpressed with different Crk mutants (Shishido *et al.*, 2001; Zvara *et al.*, 2001). To explore the functions of the SH3 linker and the proposed surface of the Crk SH3-C in further detail, we generated three types of mutants in the C-terminal region of Crk, and coexpressed these with Abl to see how they affected Abl binding and Abl transactivation. These mutants include substitutions of (i) individual proline residues of the linker, (ii) residues predicted to be on the binding surface of the Crk SH3-C, and

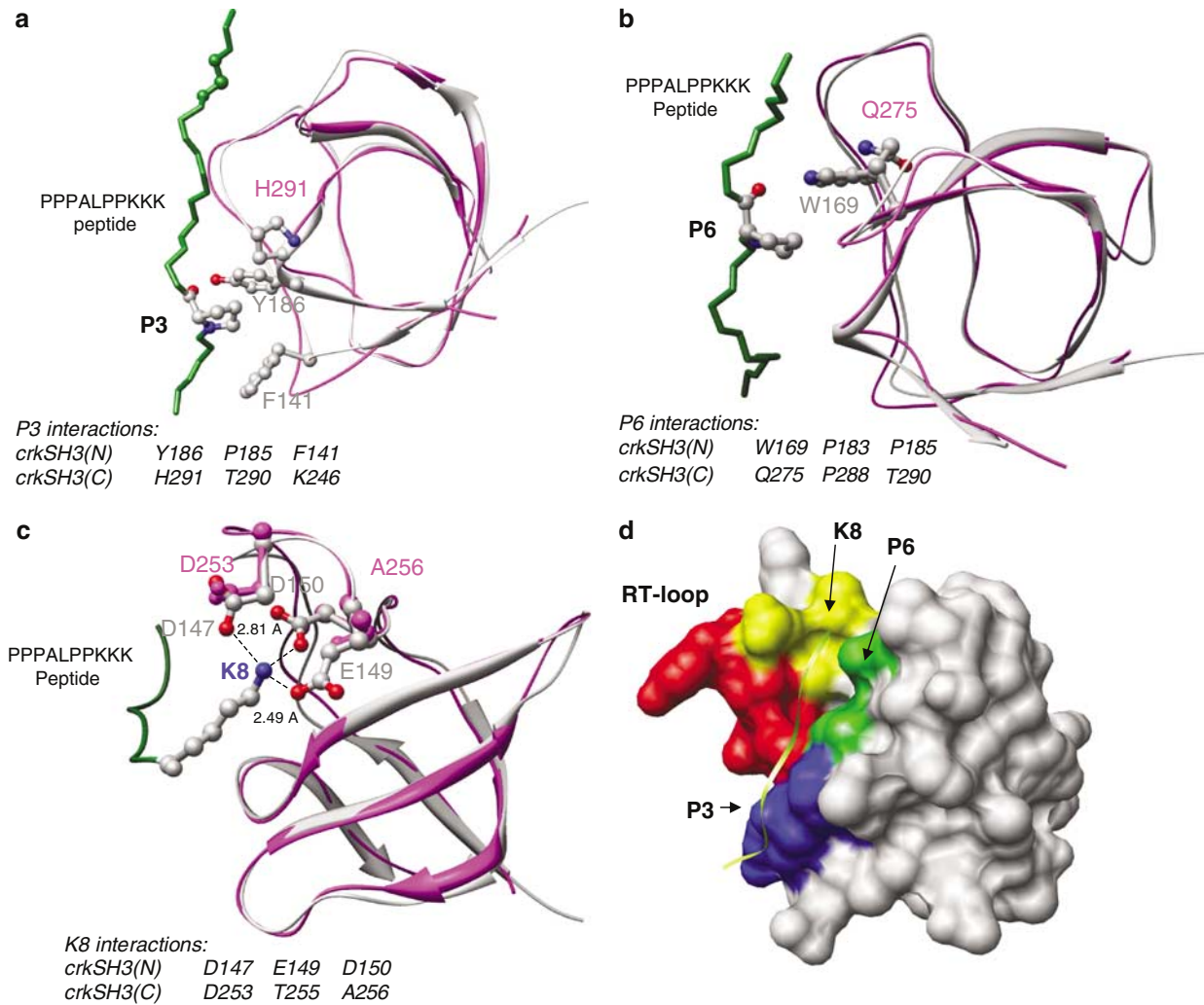


Figure 3 Peptide/SH3 interaction details. (a) Details of the interactions of the P3 residue of the PPPALPPKK peptide with the SH3-N (gray), superimposed on the corresponding residues of the SH3-C (purple). Side chains of SH3-N (gray, red for oxygen) and side chains of SH3-C (purple) are shown. (b) Details of the interactions of the P6 residue of the PPPALPPKK peptide with the SH3-N (gray), superimposed on the corresponding residues of the SH3-C (purple). Side chains of SH3-N (gray, red for oxygen) and side chains of SH3-C (purple) are shown. (c) Details of the interactions of the K8 residue of the PPPALPPKK peptide with the SH3-N (gray), superimposed on the corresponding residues of the SH3-C (purple). Side chains of SH3-N (gray, red for oxygen), side chains of SH3-C (purple), and intermolecular distances between SH3-N residues and K8 are shown. (d) Space filling model of the SH3-C with the PPPALPPKK peptide shown in the similar location to its position when binding to the SH3-N. The region that interacts with P3 of the peptide (blue), P6 (green), and K8 (yellow) are highlighted. The part of the RT loop that does not interact with PPPALPPKK and projects away from the SH3 is in red. This is the most conserved region in the alignment of Crk II and Ced-2

(iii) residues that comprise the putative RT loop of the Crk-SH3-C.

Prolines have many roles in interacting with adapter molecules, and can thereby strongly affect the regulation of these and other signaling molecules, including kinases. The best known examples of proline-binding activity are the canonical PXXP peptides that interact with most SH3 domains, and short sequences like the P²²¹YAQP²²⁵ in the Crk linker which, when phosphorylated on tyrosine, bind to SH2 domains. Proline residues in linker/connector regions have also been shown to be inhibitors in *cis* of some kinases (Macias *et al.*, 2002). For example, in Hck, the SH3 folds over and interacts intramolecularly with a small proline-containing region, blocking the kinase domain (Sicheri *et al.*, 1997).

Finally, in p47phox, an SH3 domain is inhibited from binding to interacting proteins by an intramolecular interaction with a proline-containing peptide, providing a precedent for the regulation of SH3 domain binding by such intramolecular interactions (Ago *et al.*, 1999).

Shown in Figure 4A is the Clustal W alignment of the linker regions of chicken, rat, and *Xenopus* Crk II proteins, as well as murine CrkL. The alignment of prolines is highlighted; many of these are present as PXP sequences. As the linker region of Crk II contains 10 prolines out of 49 amino acids, we decided to mutate each one individually to alanine, and test the ability of these mutants to activate Abl kinase activity. The mutants generated were P193A, P211A, P213A, P217A, P219A, P221A, P225A, P230A, and P238A

Table 1 Taxonomic alignment of the Crk-SH3-C and CrkL SH3-C domains

CLUSTAL W (1.74) multiple sequence alignment

```

mus_CrkII      PIYARVIQKRVPNAYDKTALALEVGELVKVTKINVSGQWEGECNGKRGHFPFTHVRLLDQ
hum           PIYARVIQKRVPNAYDKTALALEVGELVKVTKINVSGQWEGECNGKRGHFPFTHVRLLDQ
rat           PIYARVIQKRVPNAYDKTALALEVGELVKVTKINVSGQWEGECNGKRGHFPFTHVRLLDQ
gallus        PFYARVIQKRVPNAYDKTALALEVGELVKVTKINMSGQWEGECNGKRGHFPFTHVRLLDQ
Xenopus       PIFARVIQKRVPNAYDKTALALEVGDLVKVTKINVSGQWEGECNGKYGHFPFTHVRLLEQ
Danio         PVYARAIQKRVPNAYDKTALALEVGDVVKVTKINVNGQWEGECKGKHGHFPFTHVRLLDQ
Drosophila    PAYARVKQSRVNPAYDKTALKLEIGDIKVTKTNINGQWEGELNGKNGHFPFTHVEFVDD
Ced-2        PAKAKVTFDRVNPAYDPTQLRVKKGQTVLVTKMSNGMYKAELDGGQIGSVPHTYLRFVTA

hum_CrkL      PVFAKAIQKRVPCAYDKTALALEVGDIKVKTRMNINGQWEGEVNKRKGLFPFTHVKIFDP
DanioRerio_CrkL
PVLAKAIQKRVPCAYDKTALALEVGDIKVKTRMNINGQWEGEVNRRRGLFPFTHVKILDP
*  *:. .*** ** * * : : * : : ** : . * : : . . . : * . * . * : : :

```

Using the Clustal W 1.74 program at the EMBnet Swiss site, we aligned the SH3-C of Crk II and CrkL from several species, and found that the most conserved string of residues in Crk II was in the RT loop. This was also true when the entire Crk II alignments were examined (not shown). Shown are the SH3-C domains from the Crk II of murine (Ogawa *et al.* 1994), human (Matsuda *et al.* 1992), rat (Kizaka-Kondoh *et al.* 1996), *Gallus gallus* (Reichman *et al.* 1992), *X. laevis* (Evans *et al.* 1997), *D. rerio* (IMAGE clone AAH77088; (Lennon *et al.* 1996), and *D. melanogaster* (Galletta *et al.* 1999); the SH3-C from ced-2 of *C. elegans* (Reddien and Horvitz, 2000), and CrkL from human (ten Hoeve *et al.* 1993) and crkL *D. rerio* (IMAGE clone AAH56763; (Lennon *et al.* 1996). The PNEY sequence studied in this paper (and the aligned PCAY of crkL) is shown in gray. '*' indicates identical or equivalent residues in all sequences in the alignment, ':' indicates conserved substitutions, '.' indicates semi-conserved substitutions

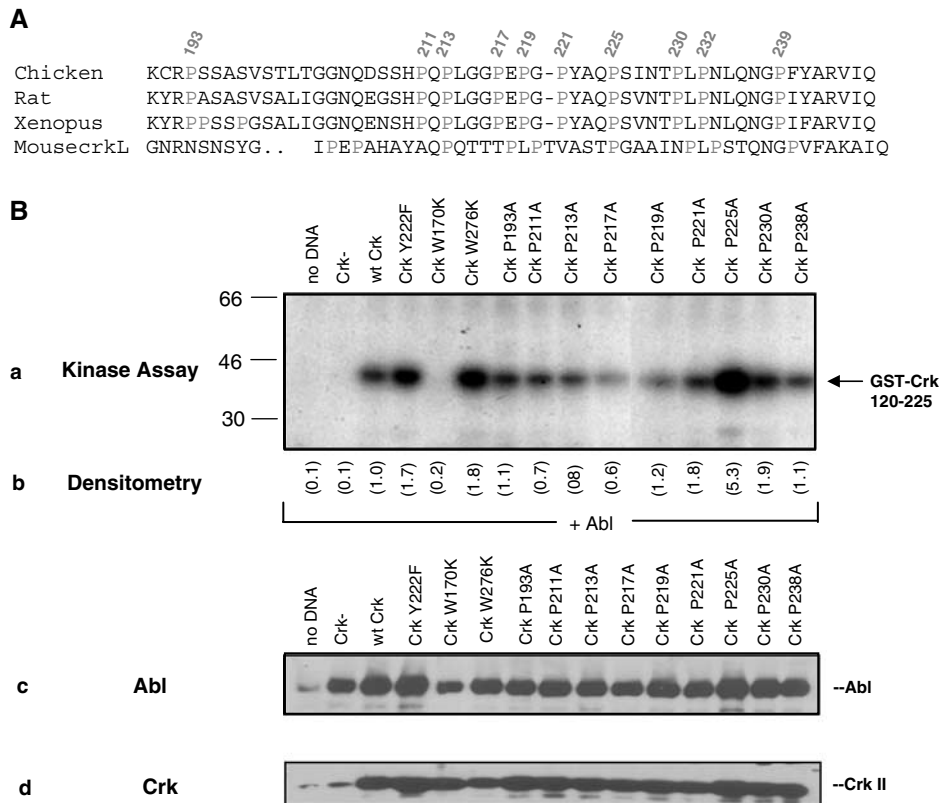


Figure 4 Proline to alanine mutations in the Crk linker. (A) Alignment of the Crk II linker from three species, together with the CrkL protein from murine. This shows the strong conservation in the linker region, including the Tyr phosphorylated by Abl, and the YXXP site which binds SH2. The Pro mutated to Ala is labeled above. (B) (a) and (b), *in vitro* kinase assay from 293T cells coexpressing Abl and Crk II constructs mutated at each of the sites shown. Kinase assays were separated by 10% SDS-PAGE and [³²P] labeled bands were detected by autoradiography. Shown at the left are sizes of protein markers, and at the right the substrate used in the kinase assay. Quantitation was on a phosphoimager (normalized to the Crk II wild-type sample). (c) and (d) Western blots of Abl and Crk expression. Equal amounts of protein from cell lysates were detected by Western blotting to confirm expression. Abl DNA was transfected in all samples except 'no DNA'

(Figure 4B). Wild-type Crk or individual Pro to Ala mutants were coexpressed with Abl in HEK 293T cells. Subsequently, detergent lysates were prepared and immunoprecipitated with anti-Crk RF51 Ab (a Crk SH2-domain specific antibody), and assayed for associated Abl kinase activity (Figure 4B a, b). For positive controls, we used Y222F, which mutates the Abl phosphorylation site, and W276K Crk, an SH3-C destabilizing mutant that we have previously shown to increase the association between Abl and Crk (Zvara *et al.*, 2001). As shown in Figure 4B a, b, most of the P to A mutants did not significantly increase Crk-associated Abl kinase activity, although consistently, P217A and P219A slightly reduced the association of Abl and Crk as indicated by the kinase pull-down assay. However, mutations in the P225 of the P²²¹YAQP²²⁵ sequence strongly increased the transactivation of Abl, as well as increasing cellular tyrosine phosphorylation

(Figure 5a; Figure 7a). Since P225 and Y222 are both a part of the pYAQP motif that interacts with the Crk-SH2 domain, they likely have a similar function in preventing SH2 docking to the Y222 when tyrosine phosphorylated. These data are consistent with the finding that the minimal SH2 recognition sequence of phospho-Y222 includes the P225, as has been reported for the Crk SH2 domain (Songyang *et al.*, 1993). Coexpression of Abl in the absence of Crk (lane 2, Figure 4A), or with W170K Crk (lane 5), an N-terminal SH3 mutant that abrogates Abl binding, produced no detectable Crk-associated Abl activity, or Abl protein (Figure 4B a, b; Figure 5d; Figure 6c). This indicates that the assay conditions specifically measure Abl activity associated with the specified Crk mutants.

Next, we studied mutants expected to disrupt the predicted binding groove of Crk SH3-C. Since the natural ligand of the Crk SH3-C is not known, we

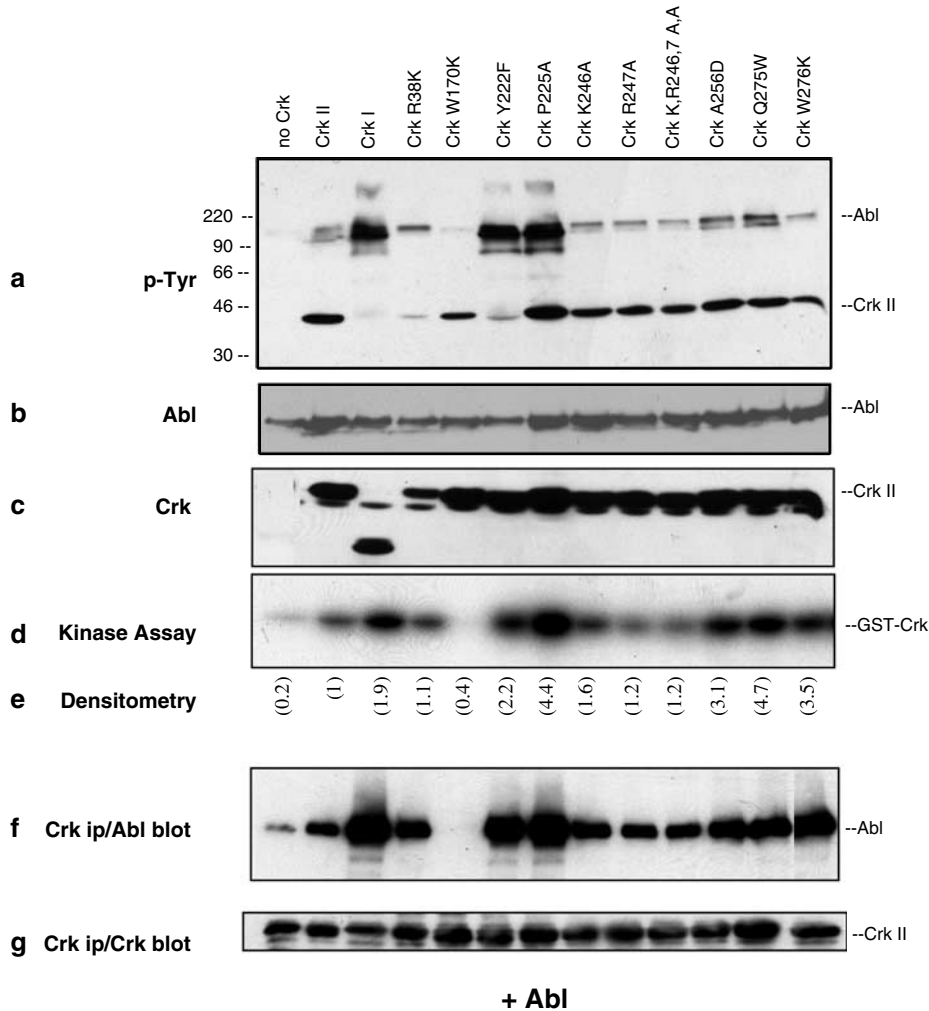


Figure 5 *In vitro* kinase assay and Western blots of Abl + Crk mutants. (a) 293T cells were cotransfected with DNAs encoding Abl plus Crk mutants as indicated. Detergent lysates were prepared 48 h later, and centrifuged to remove insoluble materials. Equal amounts of lysates were loaded on an SDS-PAGE gel and Western blotted with anti-p-Tyr antibody. (b) and (c) Western blots of lysates using the indicated antibodies. (d) Lysates were immunoprecipitated by anti-Crk antibodies, washed, and used for *in vitro* kinase assays in the presence of [³²P]ATP and GST-Crk (110–225) as exogenous substrate. Kinase assays were run on SDS-PAGE gels and quantitated on a phosphoimager. (e) Densitometry of kinase assay above (normalized to the Crk II wild-type sample). (f) and (g) Kinase assays were Western blotted with the indicated antibodies

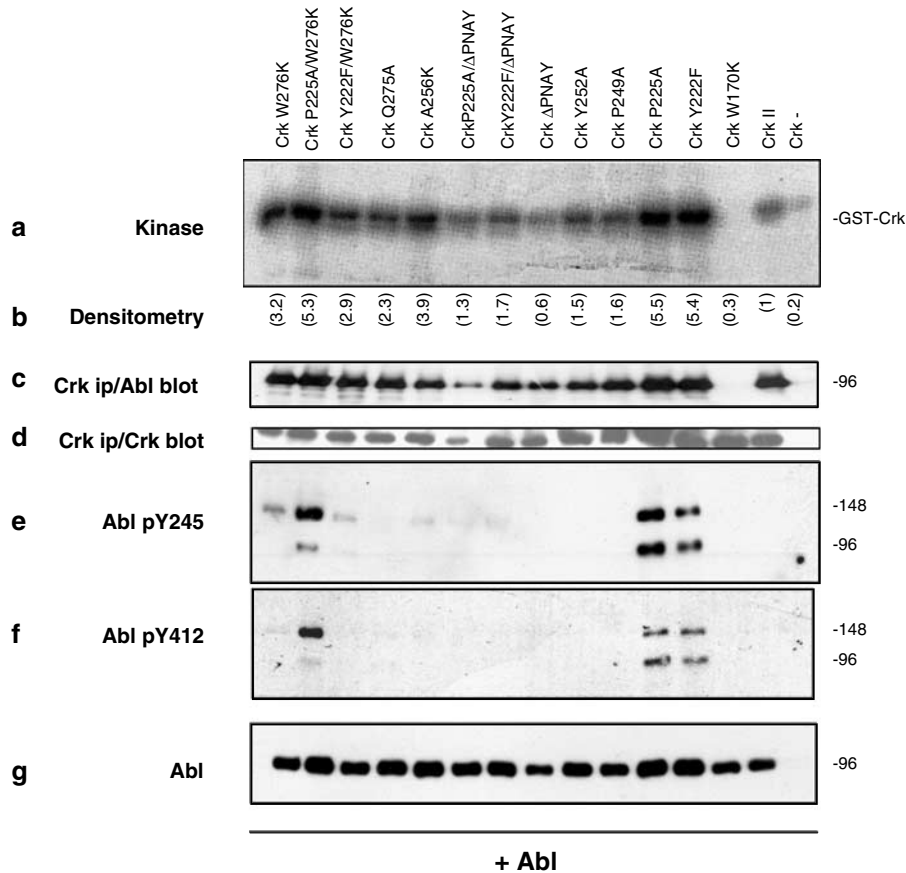


Figure 6 *In vitro* kinase assay and Western blots of Abl+Crk mutants using phospho-specific antibodies. (a) 293T cells were cotransfected with DNAs encoding Abl plus Crk mutants, as indicated. Detergent lysates were prepared 48 h later and centrifuged to remove insoluble materials. Lysates were immunoprecipitated by anti-Crk antibodies, washed, and used for *in vitro* kinase assays in the presence of [γ - 32 P]ATP and GST-Crk (110–225) as substrate. Kinase assays were run on SDS-PAGE gels and quantitated on a phosphoimager. (b) Densitometry of kinase assay above (normalized to the Crk II wild-type sample). (c) and (d) Replicate samples were immunoprecipitated and Western blotted with the indicated antibodies (e), (f) and (g) are Western blots of lysates using the indicated antibodies

mutated the corresponding amino acids that most likely replaced residues that interacted directly with the PPPALPPKK peptide in the SH3-N. These mutations include K246A, R247A, K246A/R247A, and H291A (P3-equivalent position amino acids), Q275W (P6-equivalent positions), and A256D (K8-equivalent position) (Figure 3). Subsequently, we made the additional mutations A256K and Q275A in order to mutate these residues away from the canonical SH3 residues typically found at these positions (in the case of A256, many SH3s have a D at the equivalent position, which interacts with a K or R in the K/RXXPPXXP or PXXPXK/R interacting peptide; in the case of Q275, the equivalent position is usually occupied by W, as in SH3-N). As above, CrkSH3-C mutants were co-expressed with Abl for coimmunoprecipitation and transactivation analysis (Figure 5). There was a moderate increase in Abl kinase activity when Crk II was coexpressed with Abl, compared to overexpression of Abl alone. However, the strongest activators of Abl were Crk I, Y222F, and P225A (Figure 5a). Compared to expression of Abl with wild-type Crk II, there was essentially no change in cellular phosphotyrosine levels

with the Crk II SH3-C mutants K246A, R247A, K246A/R247A, A256D, Q275W, and W276K.

Thus, mutations at residues modeled to be at the SH3-C surface did not lead to upregulation of Abl kinase activity *in vivo* compared to wild-type Crk II. However, when we examined the *in vitro* kinase activity of Crk immunoprecipitates, we found increased Abl kinase activity not only in Crk I, Y222F and P225A, but also in some of the SH3-C surface mutations, A256D, Q275W, and W276K (Figure 5d, e); the Crk II sample in lane 2 is normalized to 1). Our results with A256K and Q275A were similar to those with A256D and Q275W; neither increased *in vivo* cellular phosphotyrosine (Figure 7B a), but both showed increased *in vitro* tyrosine kinase activity (Figure 6a, b). Interestingly, when lysates of these transfected cells were co-immunoprecipitated with anti-Crk Abs, there was a correlation between the kinase activity and the extent of Abl co-immunoprecipitation (Figure 6c; Figure 5f). One possible explanation is that these mutants bind more strongly to Abl than the wild-type Crk II protein, although they do not activate its kinase activity. Thus, the increased *in vitro* kinase activity may be due to increased Abl protein complexed

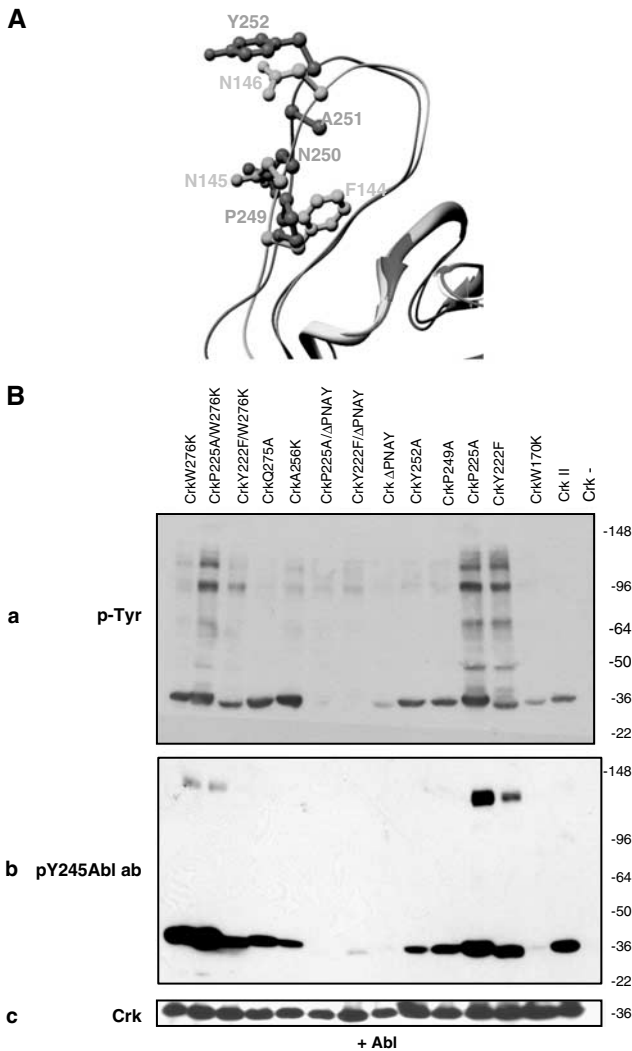


Figure 7 Predicted RT loop structure and phosphotyrosine Western blots of Abl+Crk mutants. (A) Superimposed ribbon diagrams of SH3-N (light gray) and SH3-C (dark gray). Residues of the SH3-N that do not interact with the PPPALPPKK peptide (green), and corresponding residues of the SH3-C (purple) are also shown. These residues are predicted to point away from the SH3-C. (B) (a) Equal amounts of lysates from 293T cells transfected with Abl plus Crk mutants were loaded on 8/11% step-gradient SDS-PAGE gels and Western blotted with anti-p-Tyr antibody. (b) and (c) Western blots of lysates with the indicated antibodies

with Crk in the immunoprecipitation, rather than an increase in Abl kinase specific activity.

Importantly, however, while Q275A, Q275W, A256K, A256D, and W276K Crk II may have increased the association between Crk and Abl, their mode of Abl activation was distinct from that of the Y222F and P225A mutations in the linker. In this respect, the C-terminal SH3 domain mutants did not transactivate Abl to result in increased cellular tyrosine phosphorylation (Figure 5, compare a, d; also compare Figure 6a with Figure 7B a). As a result, some linker mutants, but not SH3-C mutants tested, increase Abl kinase activity *in vivo*, it suggests that the linker region and the SH3-C perform different functions. For example, the wild-type linker may be directly inhibiting transactivation, per-

haps by binding to the kinase domain in a manner similar to the Abl kinase domain activation loop, which is also a substrate of the Abl kinase. The SH3-C may bind elsewhere on Abl (see below), or may serve to modulate the affinity of Crk II for Abl.

Abl transactivation by Crk Y222F and P225A is mediated by a PNAY sequence in the RT loop of the Crk-SH3-C

In addition to the residues of the RT loop of SH3-N that interact with K8 of the PPPALPPKK peptide, other residues point away from the binding groove and do not interact with PPPALPPKK, notably D148. Similarly, there are residues in our model of the SH3-C that also point away from the main body of the SH3-C. Interestingly, these comprise the most conserved stretch of residues between the evolutionarily distant Crk II of vertebrates and the ortholog Ced-2 protein of *C. elegans* (Table 1 and data not shown). Shown in the ribbon diagrams in Figure 7A are a number of those residues of the SH3-C (P249, N250, A251 and Y252), together with similar superimposed residues in the structure of the SH3-N (F144, N146).

We substituted a number of these residues in order to test their effect on Abl activation. When co-expressed in cells, the individual mutants P249A, Y252A and ΔPNAY had little effect on cellular phosphotyrosine compared to the wild-type Crk II protein (Figure 7B a). In addition, their effect on the *in vitro* Abl kinase assay was not dramatic (Figure 6a). This suggests that the RT loop residues are not sufficient for the direct activation of Abl by Crk II. However, we also made a number of mutants in which we combined activating mutants of Crk II with either ΔPNAY or the SH3-C structure-disrupting mutant W276K (W276 is predicted to be buried in the hydrophobic core). Interestingly, these p-Tyr Western blots show that the W276K and ΔPNAY mutations were dominant over the activating mutations; the enhanced co-immunoprecipitation and activation was either abrogated (Y222F/ΔPNAY, P225A/ΔPNAY, and Y222F/W276K) or reduced (P225A/W276K) (Figure 7B a). In addition, the enhanced co-immunoprecipitation and activation was also abrogated in the case of the Y222F/ΔPNAY and P225A/ΔPNAY mutations, and reduced for the Y222F/W276K mutant (Figure 6a–c). This suggests that the RT loop is necessary for activation of Crk II, although it is not sufficient.

Detection of Crk mutants and Abl proteins with anti-phospho-Abl antibodies

The kinase activity of Abl can be auto-inhibited through internal interactions in which its myristoylated N-terminus, and SH2 and SH3 domains bind to the two lobes of the kinase domain, termed the N- and C-terminal lobes (Nagar *et al.*, 2003). The crystal structure of the N-terminal cap region of Abl bound to its own kinase domain has shown that the auto-inhibited structure requires a P²⁴²TIY²⁴⁵ sequence, which is just N-terminal to the kinase domain. The side chain

inactive, with Crk II rather than the Abl N-terminal domains controlling/inhibiting Abl kinase activity. This also suggests that the wild-type Crk II/Abl heterodimer awaits some signal to Crk or Abl itself that results in activation of Abl. It would be interesting to test whether Δ PNAY or W276K Crk-SH3-C mutants act as dominant negative mutants for the physiological activation of the Abl or Bcr-Abl kinases.

Since it has been shown that phosphorylation of Abl Y245 relieves the intramolecular binding of the Abl P²⁴²TVY²⁴⁵ region to the Abl kinase domain, it is conceivable that phosphorylation of one or more of the PXXY sequences in Crk II could result in Abl activation. If W276K mutants of Crk II remain bound to Abl in a state in which the heterodimer complex is partially activated, they may become targets for additional phosphorylation on PXXY regions of Crk and/or Abl, without the subsequent activation of Abl. This might explain why W276K mutants had increased phosphorylation on Abl of Y412 compared to Crk II alone, on Abl and Crk of Y245 epitopes, and increased Abl *in vitro* kinase activity (i.e., possibly increased binding of Crk to Abl).

The binding of Crk to Abl could change the ability of Abl to interact with other proteins. The Abl P²⁴²TVY²⁴⁵-kinase intramolecular interaction is stabilized by the Abl SH3 domain; should the P²⁴²TVY²⁴⁵ of Abl be displaced by Crk II, then the SH3 of Abl might become available to bind to other partners. Subsequently, this could also potentially make the SH2 of Abl available as well, since it is also part of the Abl intramolecular N-terminal-to-kinase domain interaction (Nagar *et al.*, 2003).

It is already known that Abl phosphorylates Crk Y222, and autophosphorylates on Abl Y245 and Abl Y412. It would be interesting to explore whether other kinases can phosphorylate these sites, and also whether Crk can be phosphorylated at PXXY sites by Abl or another kinase. Phosphorylation of Abl at Y245 and Y412 may occur by autophosphorylation, or perhaps transphosphorylation by another Abl molecule; it has been shown that Abl can be activated by homodimerization (Smith and Van Etten, 2001). Since Src and Hck have been shown to phosphorylate and activate Abl, it is also possible that a Src family member, or another tyrosine kinase, could be involved in phosphorylating Abl or Crk when the two are in a complex (Tanis *et al.*, 2003).

Overall, these and other observations suggest that while Crk I can constitutively activate Abl kinase activity *in vivo*, Crk II activation of Abl (towards the phosphorylation of exogenous substrates) is more tightly regulated and requires a multistep process. Furthermore, it appears that any activation of Abl by Crk II that does occur requires an initiating signal in which, at the minimum, an inhibitory effect of the Crk II linker (centering on Y222) is relieved, and another activating step involving the SH3-C occurs as well. As shown in Figure 8, we propose a multistep process in the interaction and transient activation of Abl by Crk II. These include (1) the initial interaction of Crk and Abl via the SH3-N domain of Crk and the proline-rich

domain of Abl, (2) displacement of the P²⁴²TVY²⁴⁵ motif in Abl by the P²⁴⁹NAY²⁵² motif of Crk, and (3) interaction of residues surrounding the Y²²²AQP²²⁵ in the Crk II linker with the Abl kinase domain, replacing the Abl activation loop (the Abl kinase activation loop maintains Abl in the inactive configuration). Subsequently, phosphorylation by Abl of Crk at Y222, and intramolecular binding of Crk SH2 to this phosphotyrosine, leads to dissociation of Crk from Abl and signal downmodulation.

In summary, we examined the structural and functional properties of the Crk II linker and SH3-C domain to understand how they regulate the biological properties of Crk II. Using several independent criteria including tryptophan fluorescence, homology-based molecular modeling, and informatic analysis, we provide a model where the minimal functional unit of the Crk SH3-C (aa 239–293) is a modular bundle containing antiparallel β -sheets packed against each other with W276 at the hydrophobic core. However, in contrast to canonical SH3 domains, Crk SH3-C and Ced-2 SH3-C are unlikely to bind conventional PXXP-containing peptides, because the residues that are required for these interactions are mostly unconserved. Our data suggest that the SH3-C domains of Crk and Ced-2 are stable-folded entities characteristic of all known SH3 domains, but contain binding residues unique among SH3 domains. We also present evidence that the Crk-SH3-C, through a conserved PNAY sequence in the putative RT loop, is necessary for the transient activation of Abl following Crk II binding. Consistent with this study, studies by Kizaka-Kondoh *et al.* (1996) have also shown that this region of Crk is important for EGF-induced signaling to ras in rodent fibroblasts, although these investigators did not explore the role of Abl in this pathway. SH3 and SH2 domains not only bind to pY peptides and PXXP peptides intermolecularly, but they act intramolecularly in some kinases as inhibitors (Abl, Src, Hck). We hypothesize that Crk, as a protein that has been demonstrated to regulate Abl kinase activity, is using the same themes in its regulation of Abl. Thus, the method of regulation of Abl already seen intramolecularly may be conserved when Crk binds Abl, except that in the heterodimer the domains of Crk take over the regulatory roles from those of Abl. This study suggests another degree of modularity in the function of the Crk adapter protein, and a possible explanation for why the C-terminal SH3 domain is so conserved.

Materials and methods

Threading analysis, homology-derived molecular modeling, and covariation sequence analysis

A homology model of the Crk SH3-C was generated using the program Look (version 3.5; Molecular Application Group, Palo Alto, CA, USA). The template for homology modeling (Grb-2 SH3-C) was identified by threading analysis using FUGUE (Shi *et al.*, 2001) and 3D-PSSM (Kelley *et al.*, 2000). The quality of models produced by FUGUE and 3D-PSSM was evaluated with PROSA (Sippl, 1993).

Larson and Davidson (2000) used 266 SH3 domain sequences for covariation analysis, and derived a set of consensus sequences for SH3 domains. We used the first, most highly conserved consensus sequence in our alignments. A multiple sequence alignment of four sequences comprising the SH3 consensus sequence, Crk SH3-N, Crk-SH3-C, and Ced-2 SH3-C, was generated with Clustal W version 1.74. The alignment was scored for conservation of structural (hydrophobic core) and protein-binding residues.

Tryptophan fluorescence measurements

Fluorescence of constrained versus unconstrained tryptophan was measured as an indicator of protein folding. Fluorescence was measured using a Photon Technology Inc. (Lawrenceville, NJ, USA) fluorometer with a model 840 photomultiplier. Excitation was at 295 nm. Emission data were collected between 320 and 400 nm, with a step size of 0.5 nm and integration time of 0.25 s. Slit width for both excitation and emission was set at 5 nm. Measurements were made at room temperature in buffer containing 50 mM Tris pH 7.4, 150 mM NaCl, 10% glycerol, and 1 mM DTT.

Plasmids and mutagenesis

pEBB plasmids containing Crk mutant DNAs were generated using the PCR-based Quikchange™ mutagenesis system (Stratagene, La Jolla, CA, USA). The following mutants were generated: K246A, R247A, K246A/R247A, A256D, A256K, Q275W, Q275A, H291A, P193A, P211A, P213A, P217A, P219A, P221A, P225A, P230A, P238A, Y252A, and P249A. The ΔP²⁴⁹NAY²⁵² deletion mutant was generated using a modified Quikchange PCR procedure, using primers containing the desired deletion (Wang and Malcolm, 1999). The Crk II mutants, R38K, W170K, Y222F, and W276K, have been described earlier (Zvara *et al.*, 2001). For all studies, the murine Abl IV gene was used (Van Etten *et al.*, 1989).

Construction of GST-fusion proteins

cDNA amplicons encoding the linker, SH3-C and deletion mutants were generated by PCR, with primers allowing for directional cloning into the pGEX 6P-1 vector (Amersham Biosciences Corp, Piscataway, NJ, USA), for expressing GST-fusion proteins. Primer pairs were as follows:

GST-linker-SH3-C (aa 190–293); 5' AAGAATTCAAGTG TAGACCTTCCTCTGCTTCA 3' and 5' ATAGATATCT CAGCGGACATGTGTGAATGGAAAGTG 3'
GST Δ1Linker-SH3-C (aa 200–293); 5' ATGAATTCCT CTGACTGGAGGTAACCAG 3' and 5' ATAGATATCT CAGCGGACATGTGTGAATGGAAAGTG 3';
GST Δ2-Linker-SH3-C (aa 210–293); 5' ATGAATTCAC CCACAACCACTGGGTGG 3' and 5' ATAGATATCTCA GCGGACATGTGTGAATGGAAAGTG 3';
GST Δ3-Linker-SH3-C (aa 220–293); 5' ATGAATTCGGG CCCTATGCCAGCCC 3' and 5' ATAGATATCTCAGC GGACATGTGTGAATGGAAAGTG 3';
GST Δ4-Linker-SH3-C (aa 230–293); 5' ATGAATCCCG CTCCTAACCTTCAGAA 3' and 5' ATAGATATCTCA GCGGACATGTGTGAATGGAAAGTG 3'.
GST-SH3-C (aa 239–293); 5' ATGAATCTTTTATGCC CGGGTTATCCAG 3' and 5' ATAGATATCTCAGCGG ACATGTGTGAATGGAAAGTG 3';
Δ5' GST-SH3-C (aa 246–293); 5' AAGAATTCAAGCGA GTCCCTAATGCCTAC 3' and 5' ATAGATATCTCAG CCGGACATGTGTGAATGGAAAGTG 3';

GST-SH3-C (aa 239–297); 5' ATGAATCTTTTATGCC CGGGTTATCCAG 3' and 5' ATAGATATCTCATTGA TCCAGCAGGCGGACATG 3'

All inserts were cloned into the *EcoRI* and *SmaI* sites of pGEX6P-1 and sequenced to verify the integrity of the plasmid DNA.

Expression and purification of GST-fusion proteins

GST-fusion proteins were produced by standard methods from bacteria expressing inserts cloned into the pGEX 6P-1 vector (Amersham Biosciences Corp, Piscataway, NJ, USA). Briefly, plasmid constructs were transformed into competent *Escherichia coli*. Approximately 500 ml of fresh Luria-Bertani (LB) media containing ampicillin (100 μg/ml) were inoculated with a small aliquot of an overnight bacterial culture grown at 37°C. The culture was subsequently induced with 0.15 mM isopropyl-β-D-thiogalactopyranoside (IPTG) for 2 h at 37°C. The purification and elution of GST-fusion proteins was by standard protocols. The fusion proteins were liberated from GST with 2.5 U of PreScission Protease (Amersham Biosciences Corp, Piscataway, NJ, USA) at 4°C overnight. The identity and integrity of cleaved proteins was further verified using a MALDI-TOF mass spectrometer and Voyager software (Applied Biosystems, Foster City, CA, USA).

Mammalian cell transfection, electrophoresis, and kinase assays

Human embryonic kidney (HEK) 293T cells were maintained in DMEM with 10% FBS (heat inactivated) and penicillin/streptomycin. Cells were transfected with 0.5 μg of each DNA plasmid using the Lipofectamine™ transfection reagent (Invitrogen Corp., Carlsbad, CA, USA), and collected 2 days post-transfection. Cells were lysed in HNTG 1% buffer (Hepes 20 mM, pH 7.5; NaCl 150 mM; glycerol 10% and Triton X-100 1%; plus protease and phosphatase inhibitors). Lysates were examined by Western blotting and/or immunoprecipitation. Western blots were analyzed on electrophoretically resolved proteins on PVDF membranes (Millipore Corp., Billerica, MA, USA), using antiphosphotyrosine antibody PY99 (Santa Cruz Biotechnology Inc., Santa Cruz, CA, USA), anti-Abl Ab-3 (Calbiochem brand, EMD Biosciences, Inc., San Diego, CA, USA), anti-pY245, and anti-pY412 Abl IB (Cell Signaling Technology Inc., Beverly, MA, USA). The pY245 and pY412 Abl antibodies crossreact with mouse Abl. For Crk immunoblots, we used anti-Crk RF-51, a polyclonal antibody raised against the SH2 domain of Crk. Crk immunoprecipitates were performed with anti-Crk RF-51 Ab, followed by Protein A sepharose beads (Amersham Biosciences Corp., Piscataway, NJ, USA). Kinase assays were performed on Crk immunoprecipitates in kinase buffer (HNTG buffer containing 0.1% Triton X-100, 10 mM MnCl₂, 2 μg/reaction of GST-Crk amino-acid 120–225, 100 μM ATP, and 5 μCi [^γ-³²P] ATP (3000 Ci/mmol). After 30 min mixing at room temperature, reactions were terminated by the addition of SDS-PAGE sample buffer. Reactions were examined by separating proteins by SDS-PAGE and exposing the gels directly to film or to a phosphoimager plate, and by quantification using a Typhoon Storm Phosphoimager (Amersham Biosciences Corp., Piscataway, NJ, USA).

Acknowledgements

We thank Drs Cecile Bougeret, Brain Kay, Tom Muir, Stephan Feller, Sally Kornbluth, and Allan Davidson for insightful discussions and sharing unpublished data. This work was supported by a Public Health Service Award (NIH-GMS55760) to RBB and an NJCCC fellowship to Sukhwinder Singh.

References

- Ago T, Nunoi H, Ito T and Sumimoto H. (1999). *J. Biol. Chem.*, **274**, 33644–33653.
- Barber DL, Beattie BK, Mason JM, Nguyen MH, Yoakim M, Neel BG, D'Andrea AD and Frank DA. (2001). *Blood*, **97**, 2230–2237.
- Barnett P, Bottger G, Klein AT, Tabak HF and Distel B. (2000). *EMBO J.*, **19**, 6382–6391.
- Brasher BB and Van Etten RA. (2000). *J. Biol. Chem.*, **275**, 35631–35637.
- Evans EK, Lu W, Strum SL, Mayer BJ and Kornbluth S. (1997). *EMBO J.*, **16**, 230–241.
- Feller SM. (2001). *Oncogene*, **20**, 6348–6371.
- Feller SM, Knudsen B and Hanafusa H. (1994). *EMBO J.*, **13**, 2341–2351.
- Feller SM, Knudsen B, Wong TW and Hanafusa H. (1995). *Methods Enzymol.*, **255**, 369–378.
- Galletta BJ, Niu XP, Erickson MR and Abmayr SM. (1999). *Gene*, **228**, 243–252.
- Hantschel O and Superti-Furga G. (2004). *Nat. Rev. Mol. Cell Biol.*, **5**, 33–44.
- Harkioliaki M, Lewitzky M, Gilbert RJ, Jones EY, Bourette RP, Mouchiroud G, Sondermann H, Moarefi I and Feller SM. (2003). *EMBO J.*, **22**, 2571–2582.
- Hemmerlyckx B, Reichert A, Watanabe M, Kaartinen V, de Jong R, Pattengale PK, Groffen J and Heisterkamp N. (2002). *Oncogene*, **21**, 3225–3231.
- Kami K, Takeya R, Sumimoto H and Kohda D. (2002). *EMBO J.*, **21**, 4268–4276.
- Kang H, Freund C, Duke-Cohan JS, Musfelleracchio A, Wagner G and Rudd CE. (2000). *EMBO J.*, **19**, 2889–2899.
- Kay BK, Williamson MP and Sudol M. (2000). *FASEB J.*, **14**, 231–241.
- Kelley LA, MacCallum RM and Sternberg MJ. (2000). *J. Mol. Biol.*, **299**, 499–520.
- Kizaka-Kondoh S, Matsuda M and Okayama H. (1996). *Proc. Natl. Acad. Sci. USA*, **93**, 12177–12182.
- Knudsen BS, Feller SM and Hanafusa H. (1994). *J. Biol. Chem.*, **269**, 32781–32787.
- Kurakin A and Bredesen D. (2002). *J. Biomol. Struct. Dyn.*, **19**, 1015–1029.
- Kurakin AV, Wu S and Bredesen DE. (2003). *J. Biol. Chem.*, **278**, 34102–34109. Epub 2003 June 26.
- Larson SM and Davidson AR. (2000). *Protein Sci.*, **9**, 2170–2180.
- Larson SM, Di Nardo AA and Davidson AR. (2000). *J. Mol. Biol.*, **303**, 433–446.
- Lennon G, Auffray C, Polymeropoulos M and Soares MB. (1996). *Genomics*, **33**, 151–152.
- Lewitzky M, Harkioliaki M, Domart MC, Jones EY and Feller SM. (2004). *J. Biol. Chem.*, **279**, 28724–28732 Epub 2004 April 20.
- Lewitzky M, Kardinal C, Gehring NH, Schmidt EK, Konkol B, Eulitz M, Birchmeier W, Schaeper U and Feller SM. (2001). *Oncogene*, **20**, 1052–1062.
- Lowenstein EJ, Daly RJ, Batzer AG, Li W, Margolis B, Lammers R, Ullrich A, Skolnik EY, Bar-Sagi D and Schlessinger J. (1992). *Cell*, **70**, 431–442.
- Macias MJ, Wiesner S and Sudol M. (2002). *FEBS Lett.*, **513**, 30–37.
- Matsuda M, Tanaka S, Nagata S, Kojima A, Kurata T and Shibuya M. (1992). *Mol. Cell. Biol.*, **12**, 3482–3489.
- Mayer BJ, Hamaguchi M and Hanafusa H. (1988). *Nature*, **332**, 272–275.
- Mongioli AM, Romano PR, Panni S, Mendoza M, Wong WT, Musacchio A, Cesareni G and Di Fiore PP. (1999). *EMBO J.*, **18**, 5300–5309.
- Nagar B, Hantschel O, Young MA, Scheffzek K, Veach D, Bornmann W, Clarkson B, Superti-Furga G and Kuriyan J. (2003). *Cell*, **112**, 859–871.
- Ogawa S, Toyoshima H, Kozutsumi H, Hagiwara K, Sakai R, Tanaka T, Hirano N, Mano H, Yazaki Y and Hirai H. (1994). *Oncogene*, **9**, 1669–1678.
- Pires JR, Hong X, Brockmann C, Volkmer-Engert R, Schneider-Mergener J, Oschkinat H and Erdmann R. (2003). *J. Mol. Biol.*, **326**, 1427–1435.
- Reddien PW and Horvitz HR. (2000). *Nat. Cell. Biol.*, **2**, 131–136.
- Reichman CT, Mayer BJ, Keshav S and Hanafusa H. (1992). *Cell Growth Differ.*, **3**, 451–460.
- Ren R, Ye ZS and Baltimore D. (1994). *Genes Dev.*, **8**, 783–795.
- Rosen MK, Yamazaki T, Gish GD, Kay CM, Pawson T and Kay LE. (1995). *Nature*, **374**, 477–479.
- Rozakis-Adcock M, McGlade J, Mbamalu G, Pelicci G, Daly R, Li W, Batzer A, Thomas S, Brugge J, Pelicci PC, Schlessinger J and Pawson T. (1992). *Nature*, **360**, 689–692.
- Sattler M and Salgia R. (1998). *Leukemia*, **12**, 637–644.
- Shi J, Blundell TL and Mizuguchi K. (2001). *J. Mol. Biol.*, **310**, 243–257.
- Shishido T, Akagi T, Chalmers A, Maeda M, Terada T, Georgescu MM and Hanafusa H. (2001). *Genes Cells*, **6**, 431–440.
- Sicheri F, Moarefi I and Kuriyan J. (1997). *Nature*, **385**, 602–609.
- Sippl MJ. (1993). *Proteins*, **17**, 355–362.
- Smith JJ, Richardson DA, Kopf J, Yoshida M, Hollingsworth RE and Kornbluth S. (2002). *Mol. Cell. Biol.*, **22**, 1412–1423.
- Smith KM and Van Etten RA. (2001). *J. Biol. Chem.*, **276**, 24372–24379.
- Songyang Z, Shoelson SE, Chaudhuri M, Gish G, Pawson T, Haser WG, King F, Roberts T, Ratnofsky S, Lechleider RJ, Neel B, Birge RB, Fajardo JE, Chou MM, Hanafusa H, Schaffhausen B and Cantley LC. (1993). *Cell*, **72**, 767–778.
- Tanis KQ, Veach D, Duwel HS, Bornmann WG and Koleske AJ. (2003). *Mol. Cell. Biol.*, **23**, 3884–3896.
- ten Hoeve J, Morris C, Heisterkamp N and Groffen J. (1993). *Oncogene*, **8**, 2469–2474.
- Van Etten RA, Jackson P and Baltimore D. (1989). *Cell*, **58**, 669–678.
- Wang JY. (2004). *Nat. Cell Biol.*, **6**, 3–7.
- Wang B, Mysliwiec T, Feller SM, Knudsen B, Hanafusa H and Kruh GD. (1996). *Oncogene*, **13**, 1379–1385.
- Wang W and Malcolm BA. (1999). *BioTechniques*, **26**, 680–682.
- Wu X, Knudsen B, Feller SM, Zheng J, Sali A, Cowburn D, Hanafusa H and Kuriyan J. (1995). *Structure*, **3**, 215–226.
- Zvara A, Fajardo JE, Escalante M, Cotton G, Muir T, Kirsch KH and Birge RB. (2001). *Oncogene*, **20**, 951–961.